Shear wave splitting time variation by stress-induced magma uprising at Mount Etna volcano

Francesca Bianco[1], Luciano Scarfì[2], Edoardo Del Pezzo[1] & Domenico Patanè[2]

[1]Istituto Nazionale Geofisica e Vulcanologia - Osservatorio Vesuviano, Napoli (Italy)
[2] Istituto Nazionale Geofisica e Vulcanologia Sez. Catania (Italy)

Abstract

Shear wave splitting exhibits clear time variations before the July 17th – August 9th, 2001 flank eruption at Mount Etna. The normalized time delays, T_n, detected through an orthogonal transformation of singular value decomposition, exhibit a clear increase starting 20 days before the occurrence of the eruption (July 17th); the qS1 polarization direction, obtained using a 3D covariance matrix decomposition, shows a 90°-flip several times during the analyzed period: the last flip 5 days before the occurrence of the eruption. Both splitting parameters also exhibit a relaxation phase shortly before the starting of the eruption. Our observations seem in agreement with Anisotropic Poro Elasticity (APE) modelling, suggesting a tool for the temporal monitoring of the build up of the stress leading to the occurrence of the 2001 eruption at Mt. Etna.

Introduction

Shear wave splitting is the elastic analogue of the well known optical birefringence phenomenon. A shear wave entering into an anisotropic volume, is split into two quasi shear waves, qS1 and qS2, propagating with different velocities and approximately orthogonal polarizations. The splitting parameters are the time delay between qS1 and qS2 wave (hereafter referred to as T_d); and the polarization direction of the leading split (qS1) wave (hereafter referred to as *Lspd*, *Linear split polarization direction*).. The *Extensive Dilatancy Anisotropy* (*EDA*) model[*Crampin et al,* 1984], suggests that the principal source of seismic anisotropy in the crust is stress aligned fluid filled microcracks. In particular, for arrivals within the shear wave window, below about 1 km, *Lspd* is approximately parallel to the direction of the maximum compressional stress, and T_d is controlled by the distribution of densities and aspect ratios of stress-aligned, fluid-saturated, grain-boundary cracks and pore-throats present in almost all rocks at depth. The physical evolution of the EDA cracks under changing stress condition has been modeled with APE (Anisotropic Poro Elasticity) [*Zatsepin and Crampin,* 1997]. The APE deformation mechanism is controlled by the fluid migration by flow or diffusion along pressure gradients between cracks determined by the orientation of the stress field. As the stress increases in a particular direction, microcracks perpendicular to the minimum stress field increase in aspect ratio, whilst those with different orientation tend to close. The cracks are sufficiently close that they form critical systems. In the framework of APE, temporal evolution of the splitting parameters define a new class of observation that monitors changes of stress possibly related to impending earthquakes or volcanic eruptions. Interpreting changes in shear-wave splitting, *Crampin et al.* [1999] successfully stress-forecast time and magnitude of a *M*=5 earthquake in SW Iceland. Variations of shear wave splitting were observed in Southern California [*Crampin et al.* 1990; *Li et al.*, 1994]; in Southern China [*Gao et al.,* 1998]; at Parkfield, California [*Liu et al.* 1997]; in an active experiment in Southeastern Germany [*Bokelmann & Harjes,* 2000]; in Iceland [*Volti and Crampin*, 2003; *Gao and Crampin* 2004]; and for an aftershock of the Chi-Chi Earthquake in Taiwan [*Crampin and Gao*, 2005]. In volcanic areas, changes in seismic anisotropy have been measured after the 1996 eruption of Mount Ruapehu [*Miller and Savage,* 2001]; during the 1989 eruption at Mt. Etna [*Bianco et al.,* 1998]; for the September 1996 eruption at Vatnajökull, Iceland [*Volti and Crampin*, 2003]; and for the strongest earthquake (magnitude 3.6 on October 9, 1999) occurring at Mt. Vesuvius since the end of the last 1944 eruption [*Del Pezzo et al.*, 2004].

Starting from 1991 Mt. Etna experienced four major eruptions (1991, 1998, 2001 and 2002); due to its almost persistent seismic activity, it represents a natural laboratory for volcano-seismology studies. On July 17, 2001, after about three months characterized by an increase flow of lava into the SE Crater and strong Strombolian Activity, a flank eruption started. Late on July 12, 2001, there was an intense seismic swarm (over 2500 events) located in the southern part of Mt. Etna, preceding and accompanying the opening of a field of surface fractures (inset in Figure 1). The swarm continued, without any decrease in energy release, until the late hours of July 17, when at 10:00 p.m. the lava erupted from the southern tip of the fissure. This flank eruption finished on August 9, 2001. For a detailed description of the seismicity related to the 2001 eruption, as well as of the eruption itself, see *Musumeci* et al. [2004] and references therein. We measured the splitting parameters at Mt. Etna for the seismicity occurred in the period January – December 2001, including the July eruption, and found

significant variation of both T_d (depth normalized) and *Lspd* several days before the start of the flank eruption. Our observations appear to be in agreement with APE modelling, suggesting that shear wave splitting parameters may define a new class of precursors for the impending eruption at Mt. Etna.

2. Data Analysis and Results

The measurements of splitting were performed applying a rigorous selection to the seismic records, according to the following criteria: (i) clear *S*-wave onsets with s/n>6; and (ii) angles of incidence strictly inside the shear wave window (theoretically 0° - 35°, or 0° - 45° considering the effect of the shallower low-velocity layers on the ray-paths) to avoid the effect of the contamination due to the free surface interaction. As results of this selection we analyzed data collected at two digital (high dynamic) three-component seismic stations (station ESP and MNT in Figure 1). Our data-set contains 134 earthquakes recorded at ESP Station and 111 earthquakes recorded at MNT, with $1.3 \leq M \leq 3.1$ and depths in the range 3 – 20 km, collected in the period January – December 2001. Hypocentral distribution and station positions are shown in Figure 1.

Let us consider the n x 3 matrix $\boldsymbol{A}$, whose columns contain the sampled vertical and the two horizontal components, *z(t), x(t)* and *y(t),* respectively. We measured the splitting parameter T_d using the properties of the orthogonal transformations [*Shieh*, 1997]. The matrix $\boldsymbol{A}$ can be written as $\boldsymbol{A}=\boldsymbol{U}\boldsymbol{\Sigma}\boldsymbol{V}^T$, where $\boldsymbol{U}$ is a n x n orthogonal matrix, $\boldsymbol{\Sigma}$ is n x 3 diagonal matrix of eigenvalues, and $\boldsymbol{V}$ is a 3 x 3 orthogonal matrix. Using an orthogonal transformation of singular value decomposition (SVD) the components of the ground motion are decomposed into the fast *F(t)*, the slow *S(t)* and the noise *N(t)* components, according to the following: $F(t)=\lambda_1 \cdot U(t,1)$, $S(t)=\lambda_2 \cdot U(t,2)$, $N(t)=\lambda_3 \cdot U(t,3)$, and *U(t,1), U(t,2)* and *U(t,3)* are the first three columns of the $\boldsymbol{U}$ matrix. The measure of T_d is then obtained by cross correlating *F(t)* with *S(t),* on the assumption that the noise was only contained in *N(t).* T_d is then normalized for the corresponding hypocentral distance D:

$$T_n = T_d / D. \qquad (1)$$

An example of the seismic traces and of the corresponding traces obtained by applying the SVD procedure is shown in Figure 2. The APE modeling [*Crampin and Zatsepin*, 1997] considers that the normalized time delays monitor the changing stress. Band-1, the double-leaved solid angle of directions making angles 15° - 45° to the plane of the cracks, is sensitive to increasing stress. Band-2 is the solid angle of directions within 15° of the crack planes. We studied the time behavior of T_n in Band-1 and in Band-2 with respect to the ray paths. We averaged the measures in sets of nine consecutive normalized T_n, sliding each step of three events, and assigned to each average the center of the time interval between the first and the last event in the set. Results are reported in Figure 3. The error bars correspond to the standard deviation: $\sigma_{Tn}=(D^{-2}\ \sigma_{Td}^2 + D^{-4}\ \sigma_D^2 T_d^2)^{1/2}$ obtained evaluating the propagation of errors into formula (1) and assuming that the error associated with the estimate of T_d, σ_{Td}, is of the order of three samples (0.03 s, *Del Pezzo et al*., 2004), and that the error associated with the hypocentral distance, σ_D, is of the order of 0.2 km. For ESP Station, only three events showed ray paths in Band-2 for the analyzed period; consequently no evaluation was made for this low quality data set. For MNT Station the ray paths in Band-2 are mainly concentrated in the first 80 days of observations (after this period only two events with ray paths in Band-2 occurred on July 2001 and we have not reported them in Figure 3a). The distribution of T_n values in Band-2, at MNT Station, do not show any statistically significant variation. MNT Station ceased to work on July 15, having suffered damage. For both stations, the normalized time delay in Band-1 show a double pattern: a long term increase, that begins at least 20 days before the start of the effusive eruption (July 17, 2001), and a short-term decrease starting 2-3 days before the eruption. We carried out a *t-test* to show that the averages of the values before and after the apparent turning point (that we put at about 20 days before the occurrence of July 17 effusive eruption) are not different by chance. We averaged the T_n values in a time interval of 36 days before and after the turning point for the values in Band-1 at both stations (Figure 3a), showing that the averages, in all the cases, are different at a 99% confidence level.

The splitting parameter *Lspd* was obtained using a 3D covariance matrix decomposition (Born and Wolf, 1965), projecting the eigenvector related to the largest eigenvalue in the horizontal plane. The rose diagrams for the complete set of data (Figure 1) show that the qS1 polarization directions striking approximately towards NNW-SSE directions at both ESP and MNT Stations. The temporal pattern of the *Lspd* parameter is shown in the diagrams of Figure 3b. We calculated the mode of distribution for nine consecutive values, again sliding each step of three values. We used the mode (maximum of the histogram) simply to have a representation in time of the same quantity that is statistically represented through the maxima of the rose diagrams in Figure 1. We anyway tested that the mode and the unbiased estimate of the mean and standard deviation (calculated on the base of Von Mises distribution of the angular values) are close together. The time pattern at ESP (top panel) shows no significant variations in the analyzed period. At MNT (bottom panel) the pattern shows that the mode

of the qS1 polarization eigendirection exhibits two more pronounced variations (signed with circles in Figure 3b): the first at about day 90 (i.e. 100 days before July 17); the second approximately at about day 185 (5 days before July 17). We plot in the same panel the distribution of polarization directions (rose diagrams) for the pre-eruptive seismic swarm occurred on July 12 and 13 (day 185 –186); this diagram shows *Lspd* almost orthogonal to the main direction obtained for the entire analyzed period reported in Figure 1.

3. Discussions and Conclusions

We studied the time behavior of splitting parameters at Mt. Etna before, during, and after the occurrence of the July 2001 effusive eruption. In synthesis, our observations described in the previous sections show:

1. For both ESP and MNT Stations, T_n in Band-1 shows a double pattern: a long term increase, that begins at least 20 days before the starts of the effusive eruption; and a short-term decrease starting 2-3 days before the eruption (Figure 3a).
2. *Lspd* at both ESP and MNT Stations is aligned approximately in a NNW-SSE direction (Figure 1).
3. The time pattern of *Lspd* at ESP station shows no significant variations, whilst at MNT station it exhibits mainly two 90°-flip variations: the first one approximately at about day 90; the second approximately at about day 185 (Figure 3b).

Crampin [1999] suggests that increasing of the average time delay along ray paths in the double-leaved solid angle of directions Band-1 corresponds to an increase in the aspect ratio of the EDA cracks, whilst variation of time delays in Band-2 are sensitive to the crack density. In the framework of the APE modeling, the observed long-term increase of T_n at both stations indicates stress-induced increases in microcrack aspect ratios caused by the build up of stress before the eruptive phase. The observation of an abrupt short-term decrease of T_n, two to three days before the eruption, may be analogous to the T_n behavior observed immediately before several earthquakes by *Gao and Crampin* [2004]. These authors correlated the duration of the decrease with the magnitude of the event and interpreted it in terms of relaxation of local compressional stress in the preparation zone of the earthquake immediately before the earthquake occurs. By analogy, we may be observing a similar phenomenon of stress relaxation before the eruption.

The normalized splitting time delays generally assumes values less than 10 ms/km in crustal rocks [*Crampin*, 1999], but the measured T_n values at Etna always reaches values approximately twice larger as those measured elsewhere, but of the same order of those observed in Iceland [*Volti & Crampin,* 2003] and at Mt. Vesuvius [*Del Pezzo et al*., 2004]. It has been suggested that the higher T_n values in volcanic areas are probably due to the high heat flow modifying pore-fluid elasticity [*Volti & Crampin*, 2003].

The rose diagrams in Figure 1 show that at both stations *Lspd* is aligned in the same direction and it is compatible with the N-S direction of the regional stress-field acting in the area [*Patanè et al*., 2003, *Musumeci et al*., 2004]. These observations allow us to interpret the splitting parameters as due to pervasive, approximately N-S stress-aligned, fluid-filled microcracks, confirming previous observations at Mt. Etna [*Bianco et al*., 1998]. Looking at the time variation of *Lspd* (Figure 3b), changes of 90° are evident at MNT station. APE-modeling suggests that when pore-fluid pressures are low, the aligned cracks are oriented perpendicular to the direction of minimum compressional stress, hence the faster split shear wave is polarized parallel to the direction of maximum horizontal stress; when the pore fluid pressure increases reaching the overpressure regime, the effective stress-field realigns modifying the microcrack distributions, resulting in a 90°-flip of the *Lspd* [*Crampin & Zatsepin*, 1997; *Crampin*, 1999]. Consequently, we deduce from our observations that the increasing high pore-pressure induced a 90°-flip at about day 90. After day 90, the flip persists, at approximately N-S polarization, until five days before the eruption, the 90°-flip is reversed, and is accompanied by a decrease in T_n that may reflect the pressure/stress relaxation immediately before the eruption. ESP station does not show the same time pattern for *Lspd*, possibly because the overpressure regime is confined in the area of the crater and its effect decays critically with distance.

To our knowledge, previous observations of shear wave splitting parameters time variations related to volcanic eruptions are the following: *Lspd* varied showing 90°-flip before the 1995/1996 eruption at Ruapehu, [*Miller & Savage*, 2001]. T_n increased in Band-1 before the 1996 Vatnajökull eruption [*Volti and Crampin*, 2003]. T_n varied during the propagation of a dry syn-eruptive fracture for the 1989 eruption at Etna, [*Bianco et al*., 1998]. The present observation accounts for both T_n and *Lspd* time variations showing the 90°-flip and a T_n increase at long term, as well as a short–term variation that may be related to the stress-relaxation. In this framework our data agree with the APE-modelling, suggesting that the build up of the stress field increases microcrack aspect ratios till the system reaches

an over pressurized stage, accounting for the observed 90°-flip, followed by a relaxation starting shortly before the occurrence of the effusive eruption.

Acknowledgments

The authors wish to thank Stuart Crampin for stimulating discussions and comments and discerning reading of the manuscript.

References

Bianco, F., Castellano, M., Ventura, G.(1998), Structural and seismological features of the 1989 syn-eruptive NNW-SSE fracture system at Mt. Etna, *Geophys. Res. Letters*, *25,* 1545–1548.

Bokelmann, G.H., and H.P.Harjes (2000), Evidence for temporal variation of seismic velocity within the upper continental crust. *J. Geophys. Res*., 105, 23,879-23,894.

Born, M., and E. Wolf, (1965), Principles of optics. III ed.; Pergamon Press, New York,

Crampin, S., R. Evans, and B. K. Atkinson, (1984), Earthquake prediction: a new physical basis, *Geophys. J. R. Astron. Soc., 76,* 147-156,.

Crampin, S., Booth, D. C., Evans, R., Peacock, S. & Fletcher, J. B. (1990), Changes in shear wave splitting at Anza near the time of the North Palm Springs Earthquake*, J. Geophys. Res.,* 95, 11,197-11,212.

Crampin, S. & Zatsepin, S. V. (1997), Modelling the compliance of crustal rock-II. Response to temporal changes before earthquakes, *Geophys. J. Int.,129*, 495 - 506.

Crampin, S. (1999), Calculable fluid-rock interactions, *J. Geol. Soc. Lond., 156*, 501 - 514.

Crampin, S., Volti, T. and Stefansson, R. (1999), A successfully stress-forecast earthquake, Geophys. *J. Int.,138*, F1 - F5.

Crampin, S. and Y. Gao (2005), Comment on "Systematic Analysis of Shear-Wave Splitting in the Aftershock Zone of the 1999 Chi-Chi, Taiwan, Earthquake: Shallow Crustal Anisotropy and Lack of Precursory Changes," by Y. Liu, T.-L. Teng, and Y. Ben-Zion, *Bull. Seism. Soc. Am.,* in press,.

Del Pezzo, E., Bianco, F., Petrosino, S. and Saccorotti, G.(2004), Changes in the coda decay rate and shear wave splitting parameters associated to seismic swarms at Mt. Vesuvius, Italy, Bull. Seismol. Soc. Am., 94, 439 – 452.

Gao, Y. and Stuart Crampin (2004), Observations of stress relaxation before earthquakes, *Geophys. J. Int., 157*, 578-582.

Gao Y., P. Wang, S. Zheng , M. Wang, Y.Chen, and H. Zhou (1998), Temporal changes in shear-wave splitting at an isolated swarm of small earthquakes in 1992 near Dongfang, Hainan Island, southern China, *Geophys. J. Int., 135*, 102-112.

Li, Y.G. T.L. Teng, and T.L. Henyey (1994), Shear-wave splitting observations in the northern Los Angeles Basin, Southern California, *Bull. Seismol. Soc. Am. 84,*307-323.

Liu, Y., S. Crampin and I. Main (1997), Shear-wave anisotropy: spatial and temporal variations in time delays at Parkfield, Central California, *Geophys. J. Int.., 130*, 771-785.

Miller, V. and M. Savage, (2001), Changes in seismic anisotropy after volcanic eruptions: evidence from Mt. Ruapehu, *Science, 293*, 2231-2233.

Musumeci C., O. Cocina, P. De Gori, D. Patanè (2004), Seismological evidence of stress induced by dike injection during the 2001 Mt. Etna eruption, *Geophys. Res. Lett*., 31, L07617, doi:10.1029/2003GL019367

Patanè, D., De Gori, P., Chiarabba, C., Bonaccorso A., 2003, Magma ascent and the pressurization of Mount Etna's volcanic system, *Science, 299*, 2061-2063.

Shieh, C.F. (1997), Estimation of shear-wave splitting time using orthogonal transformation, *Geophysics, 62*, 657 – 661.

Volti, T., and S. Crampin, (2003), A four-year study of shear-wave splitting in Iceland: 2. Temporal changes before earthquakes and volcanic eruptions, in New insights into structural interpretation and modelling, ed. D. A. Nieuwland, *Geol. Soc. Lond., Spec. Publ. 212* 135-149. .

Zatsepin S. V, S. Crampin (1997), Modelling the compliance of crustal rock: I - response of shear-wave splitting to differential stress, *Geophys. J. Int. 129*, 477-494.

Figure Captions

Figure 1. Epicentral map and hypocentral W-E cross section of the earthquakes (gray dots) used in this study. The location of the seismic stations (open squares) of the INGV-CT permanent network is also shown (gray triangles are the two 3-C digital seismic stations MNT and ESP selected for our analysis). On the right the rose diagrams shown the NNW-SSE alignment of Lspd at both stations for the entire analyzed period. In the inset map top left, the surface fractures field (white line) and the lava flows (black) of the 2001 flank eruption are reported.

Figure 2. An example of SVD procedure to infer T_d values. The 3C signal (at the left) is decomposed into the Fast, Slow and Noise component; at the right the Cross Correlation Function between the Fast and the Slow component is shown with the indication of the measured splitting.

Figure 3. (a) Normalized time delay T_n averaged over nine consecutive points (events), sliding each step of three events. The dashed rectangle represent the window on which the *t*-test has been carried out, and the vertical arrow inside the rectangle signs the location of the turning point. (b) The mode of the distribution of *Lspd*, at both stations, for nine consecutive values, sliding each step of three values. Error bars represent the standard deviation from the unbiased mean. For MNT the rose diagram for the five days preceding the eruption is also reported. The oscillation of 90° defines the 90°-flip.The two main episodes of flip are signed with a circle.

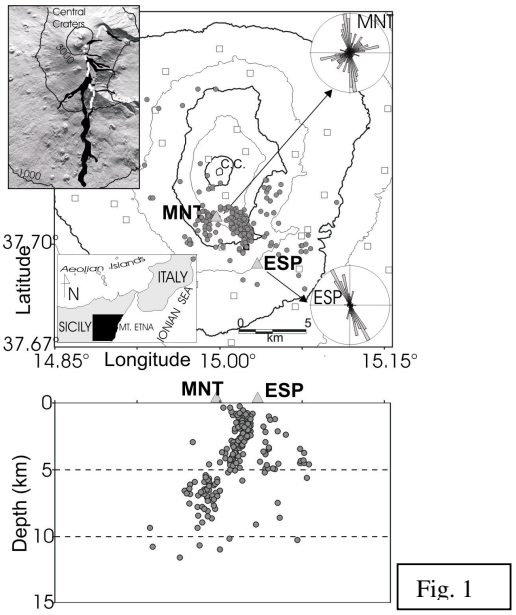

Fig. 1

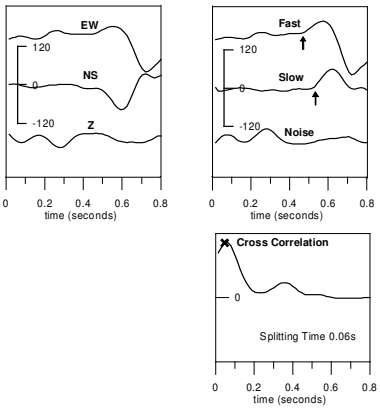

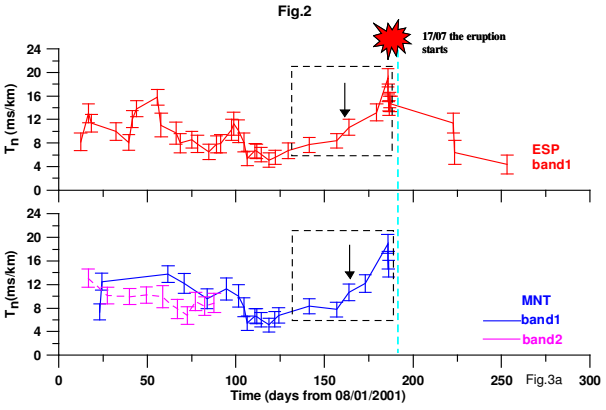

Fig.3a

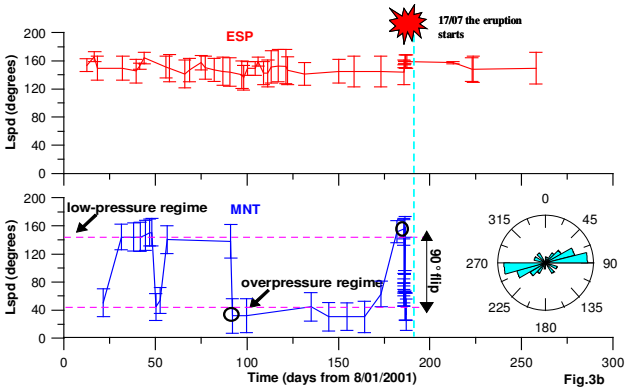
17/07 the eruption starts
ESP
Lspd (degrees)
200
160
120
80
40
0
low-pressure regime
MNT
overpressure regime
90° flip
0
45
90
135
180
225
270
315
0
50
100
150
200
250
300
Time (days from 8/01/2001)

Fig.3b